

A NEW NINE NODE DEGENERATED SHELL ELEMENT WITH ENHANCED MEMBRANE AND SHEAR INTERPOLATION

H. C. HUANG*

Tianjin University, China

AND

E. HINTON

University College of Swansea, Singleton Park, Swansea SA2 8PP, U.K.

SUMMARY

A new nine node degenerated shell element is presented in this paper. In the formulation of the new element, an enhanced interpolation of the transverse shear strains in the natural co-ordinate system is used to overcome the shear locking problem, and an enhanced interpolation of the membrane strains in the local Cartesian co-ordinate system is applied to avoid membrane locking behaviour. It is shown that the resulting element has the requisite number of zero eigenvalues and associated rigid body modes. The element does not exhibit membrane or shear locking for large span/thickness ratios. To illustrate the good performance of the new element some examples are presented including comparisons with the behaviour of the selectively integrated Lagrangian degenerated shell elements.

INTRODUCTION

Efficiency, generality and simplicity of use have ensured the continued popularity of degenerated shell elements.¹ The basic assumptions employed in degenerated shell elements are similar to those used for Mindlin plate elements. Ahmad degenerated a three dimensional brick element to a general curved shell element which has nodes only at the mid-surface. The stress in the thickness direction is assumed to be equal to zero and the element displacement field is expressed in terms of three displacements of the mid-surface and two rotations of the midsurface 'normal' and appropriate shape functions.

The original degenerated shell element performs reasonably well for moderately thick shell situations. However, for thin shells when full integration is used to evaluate the stiffness matrix, overstiff solutions are often produced due to shear and membrane locking. Attempts have been made to correct this behaviour by use of reduced or selective integration techniques.^{2,3} Such schemes are not always successful in overcoming locking behaviour and the resulting solutions may still be overstiff for problems with highly constrained boundaries, especially when coarse meshes are used. Furthermore, for problems with lightly constrained boundaries, element mechanisms or spurious zero energy modes may form. These mechanisms can spread from element

* At present a research scholar at University College of Swansea

to element causing either rank deficiency and consequently no solution, or the even more dangerous situation in which the solution obtained may be polluted by a near-mechanism.

The present degenerated shell element is developed by using

- (i) enhanced interpolation of the transverse shear strains, which has been used in several new Mindlin plate elements⁴⁻⁶
- (ii) the enhanced interpolation of the membrane strains, which is conducted in the local Cartesian co-ordinate system.

This shell element can be easily implemented by modifying existing degenerated shell programs. The main advantages of the element are that it does not lock or have any mechanisms, passes appropriate patch tests and gives generally very good behaviour.

FORMULATION OF DEGENERATED SHELL ELEMENTS

Main assumptions

Before describing the derivation of the new 9-node shell element the formulation for degenerated shell element will be reviewed.

Figure 1 shows a quadratic degenerated 9-node shell element. Two main assumptions are used in the degeneration process from solid three dimensional element to shell element. They are

1. 'Normals' to the middle surface before deformation remain straight after deformation.
2. Strain energy associated with stresses perpendicular to the local $r_1 - r_2$ surface is neglected—the normal stress component is constrained to zero and eliminated from the constitutive equations.

When applied to plates the formulation is equivalent to that presented by Mindlin⁷ in that it accounts for transverse shear deformation effects. Typically at a nodal point of a degenerated shell element there are three displacements u, v, w in the global directions x, y, z and two 'normal' rotations β_1 and β_2 .

Co-ordinate systems

The four co-ordinate systems used in the degenerated shell element formulations are shown in Figure 1 and are now defined.

1. *Global Cartesian co-ordinate systems* (x, y, z). The global Cartesian co-ordinate system is used to define the nodal co-ordinates and displacements.

2. *Curvilinear co-ordinate system* (ξ, η, ζ). The shape functions N_i are expressed in terms of the curvilinear co-ordinate system. The middle surface of the shell element is defined by the ξ and η co-ordinates. The ζ direction is only approximately normal to the shell middle surface and varies from -1 to $+1$ in the thickness direction.

3. *Local Cartesian co-ordinate system* (x', y', z'). The local Cartesian co-ordinate system is used to define local stresses and strains at any point within the shell element. At such a point the z' direction is taken to be normal to the surface $\zeta = \text{constant}$. The vector z' defines the z' direction and is obtained from the cross product of the vectors which are tangential to the ξ and η direction so that

$$\mathbf{z}' = [x_{,\xi} \ y_{,\xi} \ z_{,\xi}]^T \times [x_{,\eta} \ y_{,\eta} \ z_{,\eta}]^T \quad (1)$$

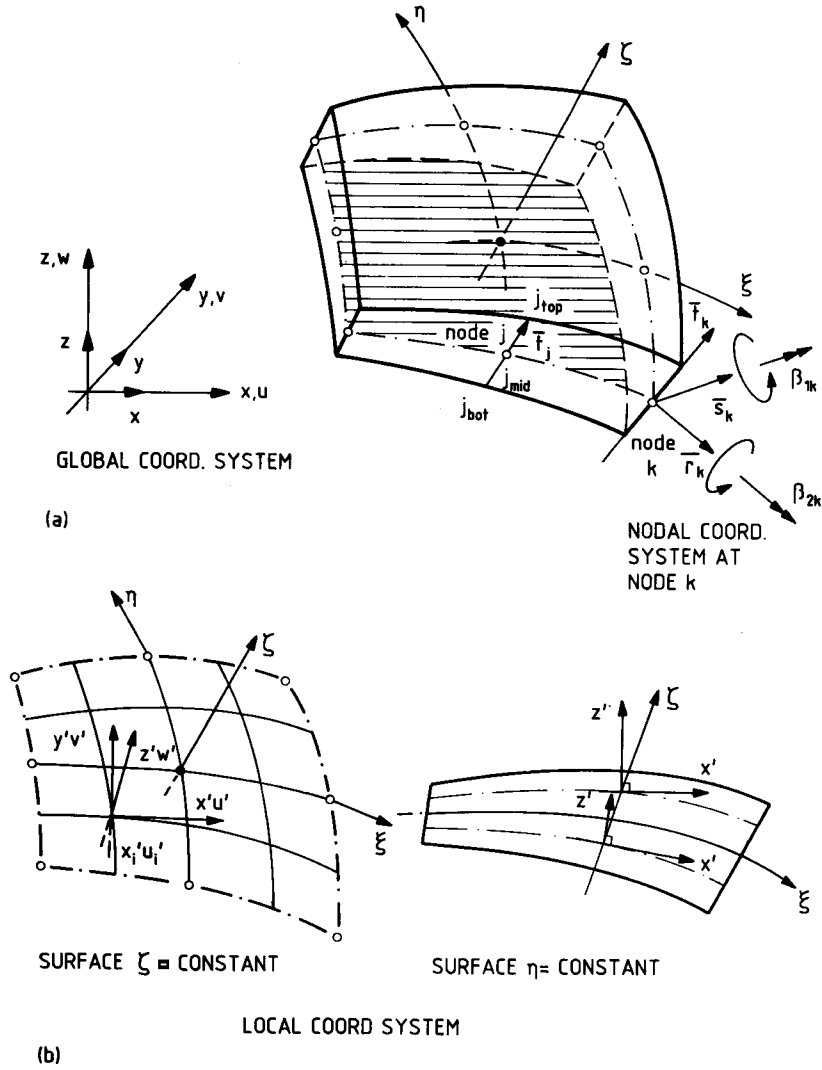


Figure 1. Co-ordinate systems: (a) nodal and curvilinear systems; (b) local system of axes

The vector \mathbf{x}' in the x direction is taken to coincide with the tangent to the ξ direction so that

$$\mathbf{x}' = [x_{,\xi} \ y_{,\xi} \ z_{,\xi}]^T. \quad (2)$$

The vector \mathbf{y}' in the y' direction is obtained by the cross product of \mathbf{z}' and \mathbf{x}' so that

$$\mathbf{y}' = \mathbf{z}' \times \mathbf{x}' \quad (3)$$

The local co-ordinate system varies throughout the shell and it is useful to define the direction cosine matrix $\boldsymbol{\theta}$ which enables transformations between the local and global co-ordinate systems to be undertaken. The direction cosine matrix is defined by the expression

$$\boldsymbol{\theta} = [\bar{\mathbf{x}}' \ \bar{\mathbf{y}}' \ \bar{\mathbf{z}}'] \quad (4)$$

where $\bar{\mathbf{x}}'$, $\bar{\mathbf{y}}'$ and $\bar{\mathbf{z}}'$ are unit vectors along the x' , y' and z' axes, respectively.

4. *Nodal Cartesian co-ordinate system* (r_k, s_k, t_k). The Cartesian co-ordinate system associated with each nodal point of the shell element has its origin at the shell midsurface. The vector \mathbf{t}_k in the t_k direction is constructed from the nodal co-ordinates of the top and bottom surfaces at node k , so that

$$\mathbf{t} = \mathbf{x}_k^{\text{top}} - \mathbf{x}_k^{\text{bot}} \quad (5)$$

where

$$\mathbf{x}_k = [x_k \ y_k \ z_k]^T$$

The vector \mathbf{r}_k is perpendicular to \mathbf{s}_k and parallel to the global xz -plane, so that

$$\mathbf{r}_k^x = \mathbf{t}_k^z, \quad \mathbf{r}_k^y = 0, \quad \mathbf{r}_k^z = -\mathbf{t}_k^x \quad (6)$$

or, if \mathbf{t}_k is coincident with the y -direction (that is $\mathbf{t}_k^x = \mathbf{t}_k^z = 0$), then

$$\mathbf{r}_k^x = -\mathbf{t}_k^y, \quad \mathbf{r}_k^y = \mathbf{r}_k^z = 0$$

where the superscripts refer to the vector components in the global co-ordinate system.

The vector \mathbf{s}_k is perpendicular to the plane defined by \mathbf{r}_k and \mathbf{t}_k , so that

$$\mathbf{s}_k = \mathbf{t}_k \times \mathbf{r}_k \quad (7)$$

The unit vectors in the directions r_k, s_k and t_k are represented by $\bar{\mathbf{r}}_k, \bar{\mathbf{s}}_k$ and $\bar{\mathbf{t}}_k$, respectively.

The vector $\bar{\mathbf{t}}_k$ defines the direction of the 'normal' at node k , which is not necessarily perpendicular to the mid-surface at k . Vectors $\bar{\mathbf{r}}_k$ and $\bar{\mathbf{s}}_k$ define the rotations β_{2k} and β_{1k} , respectively.

Element geometry

The global co-ordinates of pairs of points on the top and bottom surface at each node (see Figure 1) are usually input to define the element geometry. Alternatively, the mid-surface nodal co-ordinates and the corresponding directional thickness are provided. In the isoparametric formulation the co-ordinates of a point within the element may be expressed as

$$\begin{bmatrix} x \\ y \\ z \end{bmatrix} = \sum_{k=1}^n N_k(1-\zeta)/2 \begin{bmatrix} x_k \\ y_k \\ z_k \end{bmatrix}_{\text{top}} + \sum_{k=1}^n N_k(1-\zeta)/2 \begin{bmatrix} x_k \\ y_k \\ z_k \end{bmatrix}_{\text{bot}} \quad (8)$$

or

$$\begin{bmatrix} x \\ y \\ z \end{bmatrix} = \sum_{k=1}^n N_k \begin{bmatrix} x_k \\ y_k \\ z_k \end{bmatrix}_{\text{mid}} + \sum_{k=1}^n N_k h_k \zeta / 2 \begin{bmatrix} \bar{\mathbf{t}}_k^x \\ \bar{\mathbf{t}}_k^y \\ \bar{\mathbf{t}}_k^z \end{bmatrix} \quad (9)$$

where n is the number of nodes per element; $N_k = N_k(\xi, \eta)$ ($k = 1, \dots, n$) are the element shape functions corresponding to the surface $\zeta = \text{constant}$; h_k is the shell thickness at node k , i.e. the respective 'normal' length; ξ, η, ζ are the curvilinear co-ordinates of the point under consideration.

Displacement representation

The element displacement field can be expressed as

$$\begin{bmatrix} u \\ v \\ w \end{bmatrix} = \sum_{k=1}^n N_k \begin{bmatrix} u_k \\ v_k \\ w_k \end{bmatrix}_{\text{mid}} + \sum_{k=1}^n N_k h_k \zeta / 2 \begin{bmatrix} \bar{\mathbf{r}}_k^x & -\bar{\mathbf{s}}_k^x \\ \bar{\mathbf{r}}_k^y & -\bar{\mathbf{s}}_k^y \\ \bar{\mathbf{r}}_k^z & -\bar{\mathbf{s}}_k^z \end{bmatrix} \begin{bmatrix} \beta_{1k} \\ \beta_{2k} \end{bmatrix} \quad (10)$$

Definition of strains

In order to simplify the interpolation of the shell assumption of zero normal stress in the z' -direction ($\sigma_{z'} = 0$), the strain components should be defined in terms of the local system of axes (where z' is perpendicular to the $\xi\eta$ -plane). The local system of axes is also the most convenient system for expressing the stress components (and their resultants) for shell analysis and design. The five significant strain components are

$$\boldsymbol{\varepsilon}' = \begin{bmatrix} \varepsilon_{x'} \\ \varepsilon_{y'} \\ \gamma_{x'y'} \\ \gamma_{x'z'} \\ \gamma_{y'z'} \end{bmatrix} = \begin{bmatrix} u'_{,x'} \\ v'_{,y'} \\ u'_{,y'} + v'_{,x'} \\ u'_{,z'} + w'_{,x'} \\ v'_{,z'} + w'_{,y'} \end{bmatrix} \quad (11)$$

where u' , v' and w' are the displacement components in the local directions x' , y' and z' , respectively. These local derivatives are obtained from the global derivatives of the displacements u , v and w by the following operation

$$\begin{bmatrix} u'_{,x'} & v'_{,x'} & w'_{,x'} \\ u'_{,y'} & v'_{,y'} & w'_{,y'} \\ u'_{,z'} & v'_{,z'} & w'_{,z'} \end{bmatrix} = \boldsymbol{\theta}^T \begin{bmatrix} u_{,x} & v_{,x} & w_{,x} \\ u_{,y} & v_{,y} & w_{,y} \\ u_{,z} & v_{,z} & w_{,z} \end{bmatrix} \boldsymbol{\theta} \quad (12)$$

where $\boldsymbol{\theta}$ is a transformation matrix defined by (4). The derivatives of the displacements with respect to the global co-ordinates are given by

$$\begin{bmatrix} u_{,x} & v_{,x} & w_{,x} \\ u_{,y} & v_{,y} & w_{,y} \\ u_{,z} & v_{,z} & w_{,z} \end{bmatrix} = \mathbf{J}^{-1} \begin{bmatrix} u_{,\xi} & v_{,\xi} & w_{,\xi} \\ u_{,\eta} & v_{,\eta} & w_{,\eta} \\ u_{,\zeta} & v_{,\zeta} & w_{,\zeta} \end{bmatrix} \quad (13)$$

where \mathbf{J} is the Jacobian matrix.

$$\mathbf{J} = \begin{bmatrix} x_{,\xi} & y_{,\xi} & z_{,\xi} \\ x_{,\eta} & y_{,\eta} & z_{,\eta} \\ x_{,\zeta} & y_{,\zeta} & z_{,\zeta} \end{bmatrix} \quad (14)$$

In (13) the displacement derivatives referred to the curvilinear co-ordinates are obtained from (10), whereas the Jacobian matrix results from (9).

The strain matrix \mathbf{B} , relating the strain components in the local system to the element nodal variables, can then be constructed as

$$\boldsymbol{\varepsilon}' = \mathbf{B}\mathbf{d} \quad (15)$$

where $\boldsymbol{\varepsilon}'$ and \mathbf{d} are defined in (11) (10), respectively, and \mathbf{B} is a matrix with five rows and a number of columns equal to the number of element nodal variables.

It is convenient to write (15) in the partitioned form

$$\begin{bmatrix} \boldsymbol{\varepsilon}'_p \\ \boldsymbol{\varepsilon}'_s \end{bmatrix} = \begin{bmatrix} \mathbf{B}_p \\ \mathbf{B}_s \end{bmatrix} \mathbf{d} \quad (16)$$

in which the in-plane strains can be written as

$$\boldsymbol{\varepsilon}'_p = [u'_{,x'} \quad v'_{,y'} \quad (u'_{,y'} + v'_{,x'})]^T \quad (17)$$

and the transverse shear strains are given as

$$\boldsymbol{\varepsilon}'_s = [(u'_{,z'} + w'_{,x'}) (v'_{,z'} + w'_{,y'})]^T \quad (18)$$

Definition of stresses

Since it is assumed that there is a zero stress in the direction perpendicular to the tangent plane to the $\zeta = \text{constant}$ surface, the constitutive relationship between five stress and strain components in the local system may be written as

$$\boldsymbol{\sigma}' = \mathbf{D} \boldsymbol{\varepsilon}' \quad (19)$$

$\boldsymbol{\varepsilon}'$ is defined by (11), $\boldsymbol{\sigma}' = [\sigma_{x'} \sigma_{y'} \tau_{x'y'} \tau_{x'z'} \tau_{y'z'}]^T$ and the elasticity matrix \mathbf{D} is 5×5 matrix which can be written as

$$\mathbf{D} = \begin{bmatrix} D_{x'} & D_1 & 0 & 0 & 0 \\ D_1 & D_{y'} & 0 & 0 & 0 \\ 0 & 0 & D_{x'y'} & 0 & 0 \\ 0 & 0 & 0 & D_{x'z'} & 0 \\ 0 & 0 & 0 & 0 & D_{y'z'} \end{bmatrix} = \begin{bmatrix} \mathbf{D}_p & \mathbf{0} \\ \mathbf{0} & \mathbf{D}_s \end{bmatrix} \quad (20)$$

where for an isotropic material with elastic modulus E and Poisson's ratio ν

$$D_{x'} = D_{y'} = E/(1 - \nu^2), \quad D_1 = \nu D_{x'}, \quad D_{x'y'} = (1 - \nu)D_{x'}/2 \\ D_{x'z'} = k_1 E/2(1 + \nu), \quad D_{y'z'} = k_2 E/2(1 + \nu)$$

(N.B. The terms k_1 and k_2 are the shear correction factors associated with the transverse shear behaviour in the $x'z'$ and $y'z'$ planes, respectively.)

In partitioned form (19) can be rewritten as

$$\begin{bmatrix} \boldsymbol{\sigma}'_p \\ \boldsymbol{\sigma}'_s \end{bmatrix} = \begin{bmatrix} \mathbf{D}_p & \mathbf{0} \\ \mathbf{0} & \mathbf{D}_s \end{bmatrix} \begin{bmatrix} \boldsymbol{\varepsilon}'_p \\ \boldsymbol{\varepsilon}'_s \end{bmatrix} \quad (21)$$

in which the in-plane strains are

$$\boldsymbol{\sigma}'_p = [\sigma_{x'} \sigma_{y'} \tau_{x'y'}]^T \quad (22)$$

and the transverse shear strains are

$$\boldsymbol{\sigma}'_s = [\tau_{x'z'} \tau_{y'z'}]^T \quad (23)$$

Stiffness evaluation

In the local co-ordinate system, the total potential energy for the degenerated shell is given as

$$\pi = \frac{1}{2} \int_V \boldsymbol{\varepsilon}'_p{}^T \mathbf{D}_p \boldsymbol{\varepsilon}'_p dV + \frac{1}{2} \int_V \boldsymbol{\varepsilon}'_s{}^T \mathbf{D}_s \boldsymbol{\varepsilon}'_s dV - W \quad (24)$$

where W is the potential energy of the applied loads. In the local co-ordinate system $\boldsymbol{\varepsilon}'_p$ can be divided into two parts one associated with membrane behaviour $\boldsymbol{\varepsilon}'_m$ and one associated with bending behaviour $\boldsymbol{\varepsilon}'_b$ so that

$$\boldsymbol{\varepsilon}'_p = \boldsymbol{\varepsilon}'_m + \boldsymbol{\varepsilon}'_b \quad (25)$$

If the material properties of the shell do not vary through the shell thickness (or very symmetrically

about the midsurface) and $|\mathbf{J}|$ is supposed constant in the thickness direction, the coupling terms of $\boldsymbol{\varepsilon}'_m$ and $\boldsymbol{\varepsilon}'_b$ in (24) will disappear after the integration in the z' direction and so the total potential energy for the degenerated shell can then be directly written as

$$\pi = \frac{1}{2} \int_V \boldsymbol{\varepsilon}'_m \mathbf{D}_m \boldsymbol{\varepsilon}'_m dV + \frac{1}{2} \int_V \boldsymbol{\varepsilon}'_b \mathbf{D}_b \boldsymbol{\varepsilon}'_b dV + \frac{1}{2} \int_V \boldsymbol{\varepsilon}'_s \mathbf{D}_s \boldsymbol{\varepsilon}'_s dV - W \quad (26)$$

Upon finite element discretization and subsequent minimization of π with respect to the nodal variables \mathbf{d}_i the following equations are obtained:

$$\sum_j \mathbf{K}_{ij} \mathbf{d}_j = \mathbf{f}_i \quad (27)$$

in which the stiffness matrix \mathbf{K}_{ij} linking nodes i and j has the following typical contributions emanating from the membrane, bending and shear strain energy terms, respectively

$$\begin{aligned} \mathbf{K}_{mij} &= \int \mathbf{B}_{mi}^T \mathbf{D}_m \mathbf{B}_{mj} dV \\ \mathbf{K}_{bij} &= \int \mathbf{B}_{bi}^T \mathbf{D}_b \mathbf{B}_{bj} dV \\ \mathbf{K}_{sij} &= \int \mathbf{B}_{si}^T \mathbf{D}_s \mathbf{B}_{sj} dV \end{aligned} \quad (28)$$

Shear locking, membrane locking and selective integration

For thin shells, the transverse shear strains should tend towards zero, so that $\boldsymbol{\varepsilon}_s = 0$. Unfortunately in all of the standard quadrilateral $C(0)$ degenerated shell elements there is a tendency for shear locking in this shell situations especially if the boundaries are highly constrained. To avoid this type of behaviour, reduced and selective integration schemes have been adopted with varying degrees of success. In this paper, an enhanced interpolation of the shear strains in the natural co-ordinate system is used to produce a shear locking-free element. This approach has proved successful in a new 9-node Mindlin plate element.⁶

It is also noticed that both shear and membrane stiffnesses are of the same order of magnitude; they are both proportional to the shell thickness. Therefore, membrane locking must be expected when extremely thin shells are considered. Though, the membrane strains are still important in shells, they should not dominate the total stiffness. A selectively reduced integration scheme for the membrane stiffness has been recommended and some satisfactory results were obtained by Parisch.⁸ However, apart from the six obligatory zero energy models associated with shell rigid body movements when reduced integration of the membrane stiffness matrix is carried out three extra zero spurious energy modes are introduced due to the reduced integration. This is a serious defect. In addition, the type of selective-reduced integration suggested by Parisch can only strictly be used, when the material properties of the shell do not vary through the shell thickness (or vary symmetrically about the shell midsurface). Otherwise, the coupling terms between the membrane and the bending stiffnesses will not disappear and thus the two parts cannot be separated in order to use selective integration.

In this paper an enhanced interpolation of the membrane strains is employed in the local Cartesian co-ordinate system and neither membrane locking nor any mechanisms occur. The advantage of this approach is that it can be used for most problems with material non-linearities.

NEW DEGENERATED SHELL ELEMENT FORMULATION

Elimination of shear locking

In the curvilinear co-ordinate system the transverse shear strains $\gamma_{\xi\xi} = \gamma_{\eta\eta} \rightarrow 0$ for thin shell situations. An attempt is now made to develop a 9-node degenerated shell element in which shear locking is eliminated. The method adopted is similar to that used to develop the recently developed 4-node and 9-node Mindlin-plate elements.⁴⁻⁶

Substitute transverse shear strain fields. In the present approach a constrained functional replaces the total potential energy expression and has the form

$$\bar{\pi} = \pi + \int \lambda_{\xi\eta}(\bar{\gamma}_{\xi\xi} - \gamma_{\xi\xi}) dV + \int \lambda_{\eta\xi}(\bar{\gamma}_{\eta\eta} - \gamma_{\eta\eta}) dV \quad (29)$$

where $\lambda_{\xi\eta}$ and $\lambda_{\eta\xi}$ are Lagrangian multipliers and are independent functions. The terms $\gamma_{\xi\xi}$ and $\gamma_{\eta\eta}$ are the transverse shear strains evaluated from the displacement field. The substitute shear strains may be expressed as the following functions

$$\bar{\gamma}_{\xi\xi} = b_1 + b_2\xi + b_3\eta + b_4\xi\eta + b_5\eta^2 + b_6\xi\eta^2 \quad (30)$$

$$\bar{\gamma}_{\eta\eta} = c_1 + c_2\xi + c_3\eta + c_4\xi\eta + c_5\xi^2 + c_6\xi^2\eta \quad (31)$$

The substitute strain fields are chosen as

$$\begin{aligned} \bar{\gamma}_{\xi\xi} &= \sum_{i=1}^3 \sum_{j=1}^2 L_j(\xi) H_i(\eta) \bar{\gamma}_{\xi\xi}^{ij} \\ \bar{\gamma}_{\eta\eta} &= \sum_{i=1}^3 \sum_{j=1}^2 H_i(\xi) L_j(\eta) \bar{\gamma}_{\eta\eta}^{ij} \end{aligned} \quad (32)$$

where

$$\begin{aligned} H_1(z) &= z(z/b + 1)/2b, \quad H_2(z) = 1 - (z/b)^2, \quad H_3(z) = z(z/b - 1)/2b \\ L_1(z) &= (1 + z/a)/2, \quad L_2(z) = (1 - z/a)/2 \end{aligned} \quad (33)$$

where $a = 3^{-1/2}$, $b = 1$ and the locations of i and j are shown in Figure 2(a). Thus $\gamma_{\xi\xi}$ and $\gamma_{\eta\eta}$ have the form suggested by (30) and (31). The six unknown parameters for $\bar{\gamma}_{\xi\xi}$ are the values $\bar{\gamma}_{\xi\xi}^{ij}$ ($i = 1, \dots, 3, j = 1, 2$) at the two Gauss point locations ($\xi = \pm a$) at the three lines $\eta = b$, $\eta = 0$ and $\eta = -b$. Thus $\bar{\gamma}_{\xi\xi}$ is linear in ξ and quadratic in η . Similarly, the six unknown parameters defining $\bar{\gamma}_{\eta\eta}$ are the values $\bar{\gamma}_{\eta\eta}^{ij}$ ($i = 1, \dots, 3, j = 1, 2$) at two Gauss point locations ($\eta = \pm a$) at the three lines $\xi = b$, $\xi = 0$ and $\xi = -b$. Thus $\bar{\gamma}_{\eta\eta}$ is linear in η and quadratic in ξ (see Figure 2(b)).

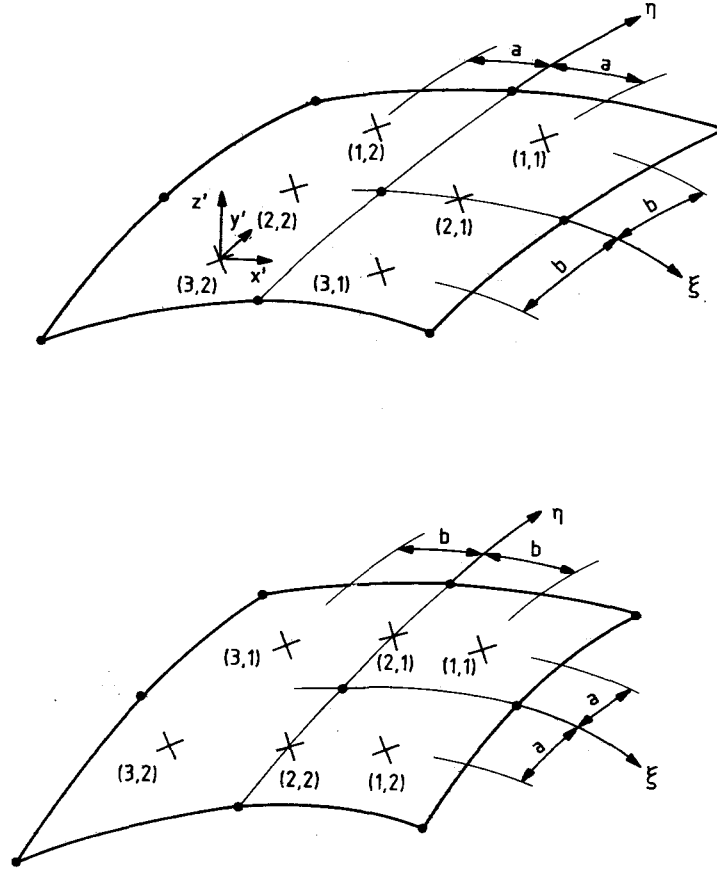
In order to eliminate shear locking behaviour, the constraints on the shear strains should not be too strong, and consequently $\lambda_{\xi\xi}$ and $\lambda_{\eta\eta}$ are chosen as Dirac delta functions of the following form:

$$\begin{aligned} \lambda_{\xi\xi} &= \lambda_{\xi\xi}^{11} \delta(a - \xi) \delta(b - \eta) + \lambda_{\xi\xi}^{12} \delta(a + \xi) \delta(b - \eta) + \lambda_{\xi\xi}^{21} \delta(a - \xi) \delta(\eta) + \lambda_{\xi\xi}^{22} \delta(a + \xi) \delta(\eta) \\ &\quad + \lambda_{\xi\xi}^{31} \delta(a - \xi) \delta(b + \eta) + \lambda_{\xi\xi}^{32} \delta(a + \xi) \delta(b + \eta) \end{aligned} \quad (34)$$

$$\begin{aligned} \lambda_{\eta\eta} &= \lambda_{\eta\eta}^{11} \delta(a - \eta) \delta(b - \xi) + \lambda_{\eta\eta}^{12} \delta(a + \eta) \delta(b - \xi) + \lambda_{\eta\eta}^{21} \delta(a - \eta) \delta(\xi) + \lambda_{\eta\eta}^{22} \delta(a + \eta) \delta(\xi) \\ &\quad + \lambda_{\eta\eta}^{31} \delta(a - \eta) \delta(b + \xi) + \lambda_{\eta\eta}^{32} \delta(a + \eta) \delta(b + \xi) \end{aligned} \quad (35)$$

Upon substitution of (32)–(35) into (29) and upon subsequent realization of the stationarity of $\bar{\pi}$, the following relationships are obtained:

$$\begin{aligned} \bar{\gamma}_{\xi\xi} &= \gamma_{\xi\xi} \quad \text{at } (i = 1, \dots, 3, j = 1, 2) \\ \bar{\gamma}_{\eta\eta} &= \gamma_{\eta\eta} \quad \text{at } (i = 1, \dots, 3, j = 1, 2) \end{aligned} \quad (36)$$

Figure 2(a). Interpolation points (i, j)

If (36) can be satisfied in advance then it is possible to work with the following functional:

$$\pi = \frac{1}{2} \int_V \boldsymbol{\varepsilon}_p^T \mathbf{D}_p \boldsymbol{\varepsilon}_p dV + \frac{1}{2} \int_V \bar{\boldsymbol{\varepsilon}}_s^T \mathbf{D}_s \bar{\boldsymbol{\varepsilon}}_s dV - W \quad (37)$$

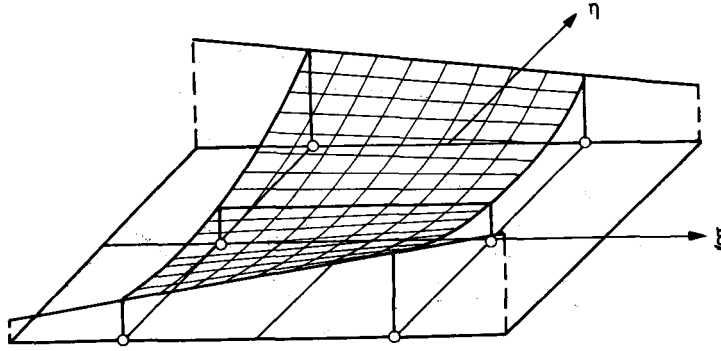
in which

$$\bar{\boldsymbol{\varepsilon}}_s = [\bar{\gamma}_{x'z'} \quad \bar{\gamma}_{y'z'}]^T \quad (38)$$

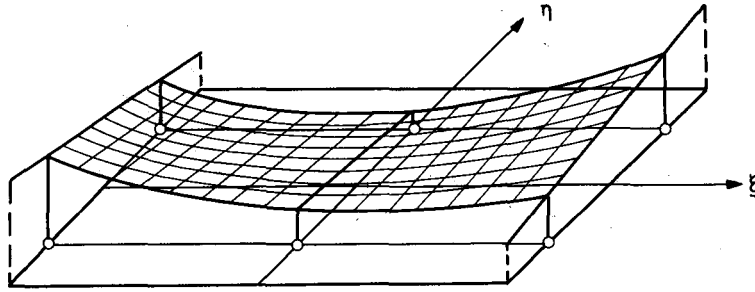
where $\bar{\gamma}_{x'z'}$ and $\bar{\gamma}_{y'z'}$ are obtained from $\bar{\gamma}_{\xi\zeta}$ and $\bar{\gamma}_{\eta\zeta}$ given by (32) and (33), respectively, by tensor transformation.

Enhanced interpolation of the membrane strains

Both the membrane stiffness and the shear stiffness are usually of the same order of magnitude. However, membrane locking is somewhat different to shear locking in which the transverse shear strains in the finite element method cannot tend towards zero with decreasing thickness as they should according to thin shell theory. In shells the stiffness associated with the membrane strain energy, though important, especially when the shell thickness becomes very small, should not dominate the total stiffness. It is known that the membrane strains can only be separated



INTERPOLATION FOR $\gamma_{\xi\xi}$, $\epsilon_{mx'x'}$ AND $\frac{1}{2}\epsilon_{mx'y'}$



INTERPOLATION FOR $\gamma_{\eta\eta}$, $\epsilon_{my'y'}$ AND $\frac{1}{2}\epsilon_{mx'y'}$

Figure 2(b). Interpolation functions ($a = 3^{-1/2}$, $b = 1$)

from the bending strains in the local Cartesian co-ordinate system. Therefore, it is expected that the use of an enhanced interpolation of the membrane strains in the local Cartesian co-ordinate system can help to eliminate membrane locking behaviour.

Expression of membrane strains. In the local co-ordinate system, the in-plane displacements can be expressed as

$$\begin{aligned} u' &= u'_0 + z'\theta_{x'} \\ v' &= v'_0 + z'\theta_{y'} \end{aligned} \quad (39)$$

where u'_0 and v'_0 are displacements in the mid-surface of the element. For the quadratic isoparametric element, the u'_0 and v'_0 should be also quadratic in x' and y' ($z' = 0$). The membrane strains are thus obtained from (39), and can be written as

$$\epsilon_{mx'x'} = u'_{0,x'} = \epsilon_{mx'x'}(1, x', y', x'y', x'(y')^2, (y')^2) \quad (40)$$

$$\varepsilon_{my'y'} = v'_{0,y'} = \varepsilon_{my'y'}(1, x', y', x'y', (x')^2 y', (x')^2) \quad (41)$$

$$\varepsilon_{mx'y'} = u'_{0,y'} + v'_{0,x'} = \varepsilon_{mx'y'}(1, x', y', x'y', (x')^2 y', (x')^2 y', x'(y')^2, (y')^2) \quad (42)$$

Therefore, for $\varepsilon_{mx'x'}$, $\varepsilon_{my'y'}$ and $\varepsilon_{mx'y'}$ the interpolation is as follows:

$$\bar{\varepsilon}_{mx'y'} = \sum_{i=1}^3 \sum_{j=1}^2 L_j(\xi) H_i(\eta) \bar{\varepsilon}_{mx'y'}^{ij} \quad (43)$$

$$\frac{1}{2} \bar{\varepsilon}_{mx'y'} = \sum_{i=1}^3 \sum_{j=1}^2 L_j(\xi) H_i(\eta) \bar{\varepsilon}_{mx'y'}^{ij} / 2 \quad (44)$$

$$\bar{\varepsilon}_{my'y'} = \sum_{i=1}^3 \sum_{j=1}^2 H_i(\xi) L_j(\eta) \bar{\varepsilon}_{my'y'}^{ij} \quad (45)$$

$$\frac{1}{2} \bar{\varepsilon}_{my'y'} = \sum_{i=1}^3 \sum_{j=1}^2 H_i(\xi) L_j(\eta) \bar{\varepsilon}_{my'y'}^{ij} / 2 \quad (46)$$

where $H_i(z)$ and $L_j(z)$ have the same meaning as in (32) and $a = 3^{-1/2}$ and $b = 1$.

Thus $\varepsilon_{mx'x'}$ and $\varepsilon_{mx'y'}$ are linear in x' and quadratic in y' , $\varepsilon_{my'y'}$ and $\varepsilon_{mx'y'}$ are linear in y' and quadratic in x' (see Figure 2b). Finally, the in-plane shear strain is quadratic in both directions, that is

$$\bar{\varepsilon}_{mx'y'} = \frac{1}{2} \sum_{i=1}^3 \sum_{j=1}^2 L_j(\xi) H_i(\eta) \bar{\varepsilon}_{mx'y'}^{ij} + \frac{1}{2} \sum_{i=1}^3 \sum_{k=1}^2 H_i(\xi) L_k(\eta) \bar{\varepsilon}_{mx'y'}^{ik} \quad (47)$$

New 9-noded degenerated shell element

In the formulation of the new 9-noded degenerated shell element the membrane and shear strains are interpolated from identical sampling points, but in different co-ordinate systems: one is in the local Cartesian co-ordinate system, the other is in the natural co-ordinate system. Table I gives the details of the modification of the shell strains.

REINTERPRETATION OF QUADRATIC SELECTIVELY INTEGRATED SHELL ELEMENT

It is possible to view selectively integrated elements as specialized examples of elements with enhanced membrane and shear interpolation. For example, an element with a reduced integration scheme used for the membrane and shear stiffness matrix, can be interpreted as one in which the strains are interpolated from the reduced (2×2) Gauss–Legendre points with a full integration rule then being used to evaluate the total stiffness matrix. In the new shell element, however, the shear and membrane strains are interpolated from two Gauss points in ξ and three points $(b, 0, -b)$ in η for $\bar{\gamma}_{\xi\zeta}$, $\bar{\varepsilon}_{mx'x'}$ and $\frac{1}{2} \varepsilon_{mx'y'}$ and three points $(b, 0, -b)$ in ξ and two Gauss points in η for $\bar{\gamma}_{\eta\zeta}$, $\bar{\varepsilon}_{my'y'}$ and $\frac{1}{2} \bar{\varepsilon}_{mx'y'}$ with full integration.

The difference between the interpolations of the membrane and transverse shear strains in the new shell element is that for the membrane strains the interpolation is conducted in the local Cartesian co-ordinate system whereas for the transverse shear strains the interpolation is conducted in the natural co-ordinate system. If the value $b = (\frac{3}{8})^{1/2}$ is taken in Figure 2(a), for shells in which the material properties do not vary through the thickness (or vary symmetrically about the shell midsurface), then the interpolation of the membrane strains is equivalent to use of a special reduced integration for the membrane stiffness. Thus, a $2(\text{in } x') \times 3(\text{in } y')$ reduced integration scheme is used for $\xi_{mx'x'}$ and $\frac{1}{2} \varepsilon_{mx'y'}$ and a $3(\text{in } x') \times 2(\text{in } y')$ reduced integration scheme

Table I. Modifications of the new shell element strains


Strains			
In global co-ordinate system	$\varepsilon_{ij} = \frac{1}{2}(u'_{i,j} + u'_{j,i}) = \mathbf{B}\mathbf{d}$		
Transformation into	Local co-ordinate system	Natural co-ordinate system	
	$\varepsilon'_{i'j'} = \frac{\partial x^i}{\partial x^{i'}} \frac{\partial x^j}{\partial x^{j'}} \varepsilon_{ij}$	$e_{\alpha\beta} = \frac{\partial x^i}{\partial \xi^\alpha} \frac{\partial x^j}{\partial \xi^\beta} \varepsilon_{ij}$	
Interpolation	ε'_m	ε'_b	e_s
			$\bar{\gamma}_{\xi\xi}$
	$\bar{\varepsilon}_{mx'x'}$		
	$\frac{1}{2}\bar{\varepsilon}_{mx'y'}$		
Interpolation	$\bar{\varepsilon}_{my'y'}$		$\bar{\gamma}_{\eta\xi}$
	$\frac{1}{2}\bar{\varepsilon}_{mx'y'}$		
Transformation into local co-ordinate system	$\bar{e}_{\xi i'j} = \frac{\partial \xi^\alpha}{\partial x^{i'}} \frac{\partial \xi^\beta}{\partial x^{j'}} e_{\alpha\beta}$		
Integration in full	$\varepsilon' = \bar{\varepsilon}'_m + \varepsilon'_b + \bar{\varepsilon}'_s = \bar{\mathbf{B}}'\mathbf{d}$ $\mathbf{K} = \int_V \mathbf{B}'^T \mathbf{D} \mathbf{B}' dV$		

Table II. Investigated quadratic degenerated shell elements

Element models	Interpolation rule			Mechanisms
	Shear stiffness	Bending stiffness	Membrane stiffness	
1 QUAD9*R			2 × 2	3
2 QUAD9*			2 × 3/3 × 2	0
3 QUAD9**	2 × 3/3 × 2 +	3 × 3	2 × 3/3 × 2 + +	0
4 QUAD9*F			3 × 3	0
5 QUAD9RR			2 × 2	4
6 QUAD9R	2 × 2	3 × 3	2 × 3/3 × 2	1
7 QUAD9RF			3 × 3	1

+ the enhanced interpolation of shear strains in ξ - η co-ordinate system.

+, + + the interpolation with $b = 1$, otherwise, $b = (\frac{2}{3})^{-1/2}$

is used for $\bar{\epsilon}_{my'y'}$ and $\frac{1}{2}\bar{\epsilon}_{mx'y'}$. So, in other words, because the integration of the membrane stiffness has been reduced in one direction, the membrane locking behaviour is eliminated.

Details of the interpolation rule used in the interpolation of the several element models are given in Table II.

NUMERICAL APPLICATIONS

Introduction

Some numerical examples are now presented in which QUAD9**, the new element, is used. Comparisons are also provided with the performance of several other models of the 9-node Lagrangian element.

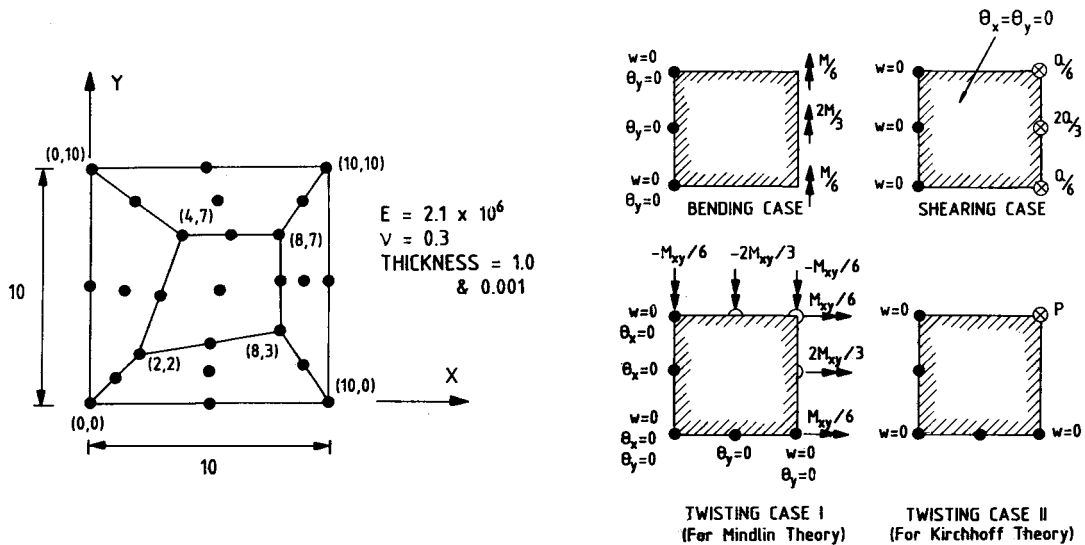
Numerical tests for element characteristics

Eigen-analysis of the stiffness matrix. From an eigen-analysis of stiffness matrix for the new element QUAD9** it was found that there are only six zero eigenvalues each associated with a rigid mode. Consequently, no mechanisms are present in QUAD9**. Some details about the numbers of spurious modes in the other models are listed in Table II.

Bending and plane stress patch tests. Patch tests performed on shells for meshes of arbitrary quadrilaterals of the type shown in Figure 3(a) indicate that QUAD9** and the other elements in Table II can represent fields of constant moment, twist or transverse shear forces and constant in-plane tension and shear forces for both thick and thin cases.

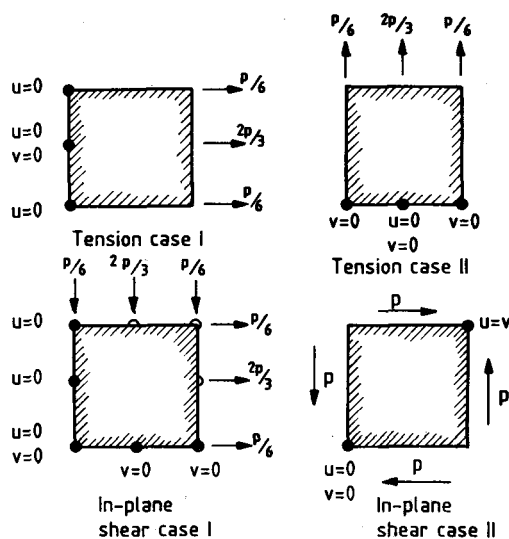
The results for bending patch tests are identical to those obtained with a recently developed Mindlin plate element.⁶ The loading cases are shown in Figure 3(b).

Plane stress patch tests were then carried out. For the tension patch tests, distributed edge tension forces of constant intensity are applied in both the cases shown in Figure 3(c). Linear



(a) PATCH OF ELEMENTS USED

(b) LOAD CASES



(c) LOAD CASES

Figure 3. Patch test. A patch of elements is considered in the load cases shown: the patch test is passed

displacements and constant tensile stresses are obtained. In the plane stress shear patch test, for case I, two adjacent edges are constrained and compressive and tensile forces of constant intensity are applied along the opposite edges as shown in Figure 3(c). For case II, distributed tangential edge forces of constant intensity are applied as shown in Figure 3(c). For both cases, constant in-plane shear stresses are obtained.

All of the element models given in the Table II can pass these patch tests.

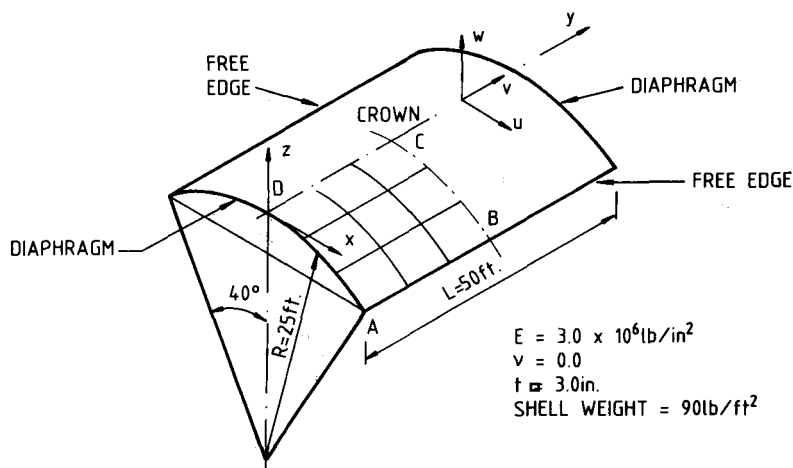


Figure 4. Cylindrical shell roof configuration (3×3 grid shown)

Table III. Membrane locking tests

	Cylindrical shell roof		Pinched cylindrical shell
Mesh	4 × 4		8 × 8
Models	w_B	w_C	w_C
1 QUAD9*R	-3.6407	0.5455	163.675
2 QUAD9*	-3.6157	0.5401	163.588
3 QUAD9**	-3.6152	0.5404	163.863
4 QUAD9*F	-2.9769	0.3771	139.250
5 QUAD9RR	-3.6641	0.5503	165.538
6 QUAD9R	-3.6388	0.5449	164.638
7 QUAD9RF	-2.9923	0.38051	140.338
Exact deep shell	-3.6100	0.54070	164.240
Shallow shell	-3.7000	0.55200	- - - -

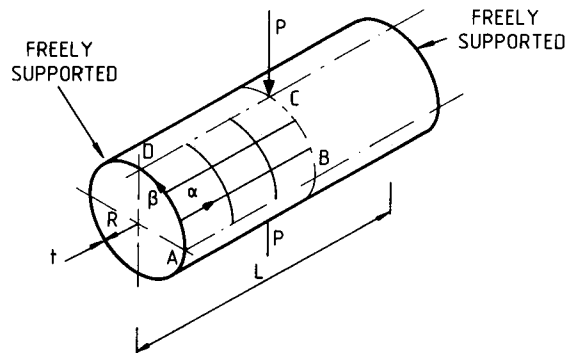


Figure 5. Pinched cylindrical shell configuration

Shear locking tests. In the shear locking test a symmetric quadrant of a uniformly loaded square, clamped plate is idealized using various 2×2 meshes of the type described in Reference 6. There is no locking behaviour and the transverse central displacement becomes asymptotic to the theoretical solutions for plates with decreasing thickness.

Membrane locking tests. In the membrane locking tests, two examples are used. They are the well-known cylindrical shell roof problem and the pinched cylindrical shell problem.

The cylindrical shell roof shown in Figure 4 is now considered. The shell which is simply supported (diaphragm) along two edges and free along the other two edges, has been examined by a number of investigators.

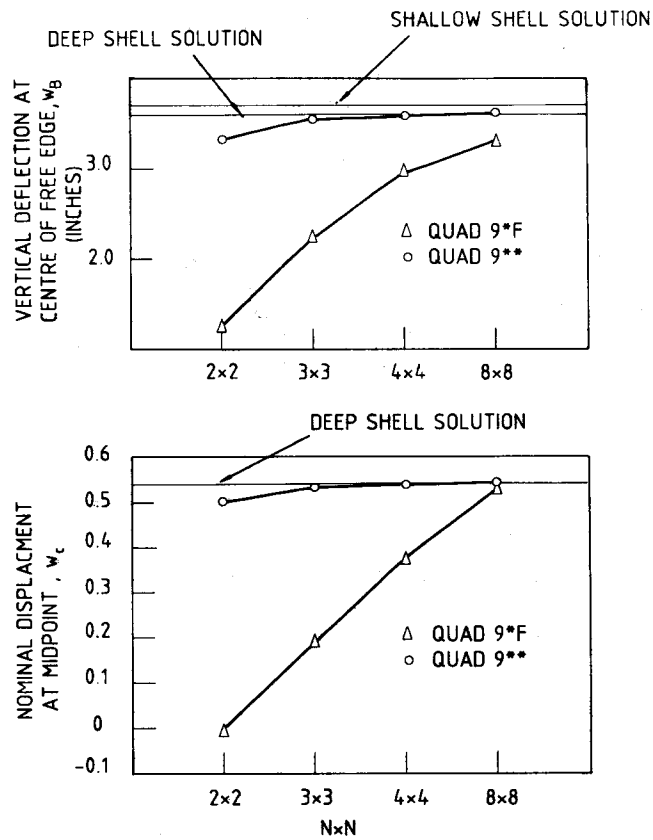


Figure 6. Cylindrical shell roof subjected to self weight

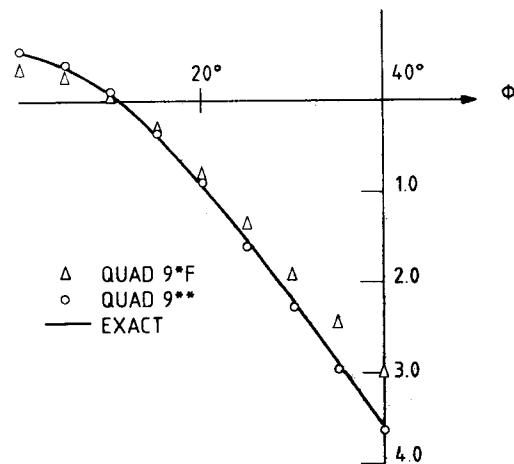


Figure 7. Vertical displacement of central section for cylindrical shell roof

The pinched cylinder problem is shown in Figure 5. The ends of the cylinder are simply supported and it is loaded by two opposite concentrated forces.

In Table III, it is noticed that over stiff solutions are obtained using the models with full integration (QUAD9*F, QUAD9RF) for the membrane stiffness, whereas with reduced integration, much more accurate solutions are obtained and with the enhanced interpolation of the membrane strains for both $b = 1$ (QUAD9**) and $b = (\frac{2}{3})^{-1/2}$ (QUAD9*), the accuracy is almost the same as that obtained with reduced integration.

In Figures 6–9, it is shown that there are substantial differences between solutions with full integration for the membrane stiffness and those with the unidirectional reduced integration, especially for coarse meshes. These differences highlight the influence of membrane locking in the degenerated shell element.

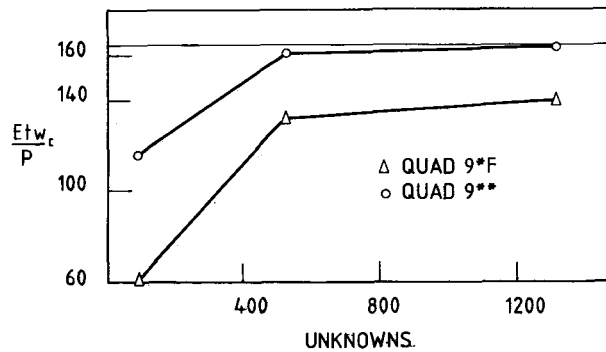


Figure 8. Convergence for pinched cylindrical shell

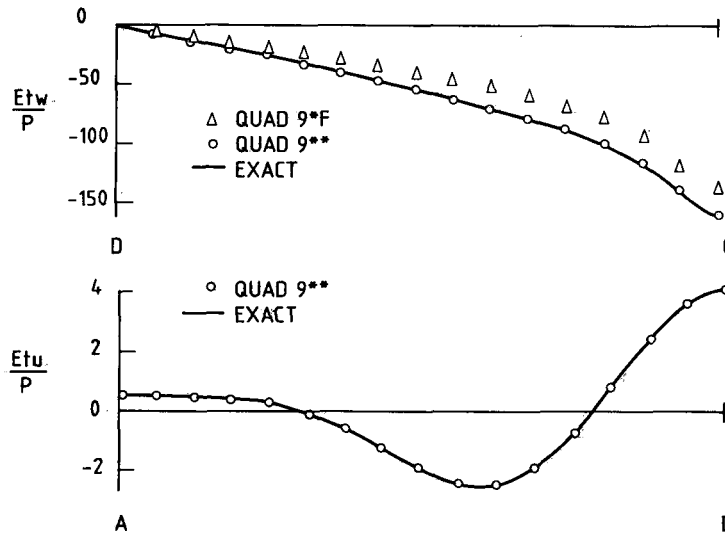


Figure 9. Displacement distributions for pinched cylindrical shell

Clamped hyperbolic paraboloid shell

Figure 10 shows a clamped hyperbolic paraboloid shell in which the real shell geometry can be exactly represented by the degenerated elements. Here

$$z = xy/c, \quad c = 250$$

$$t = 1/(x^2 + y^2 + c^2)^{1/2}[-y, -x, c], \quad \text{at point } (x, y)$$

The shell is subjected to a uniform pressure. The deflection along the centre-line is plotted in Figure 11 and compared to the exact solution.⁹ Table IV provides an interesting comparison of transverse displacements obtained with QUAD9*F and value obtained with QUAD9**. The displacements along the central line obtained using QUAD9** are almost the same as those given by QUAD9*F. This means that in the hyperbolic shell, the influence of membrane locking is not important. (Note that the mid-surface of the hyperbolic shell is a bilinear function, so for the four-node element,⁵ the influence of membrane locking is also not important.)

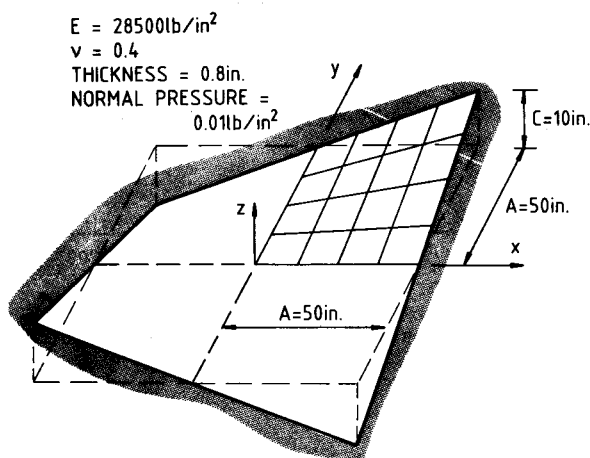


Figure 10. Clamped hyperbolic shell

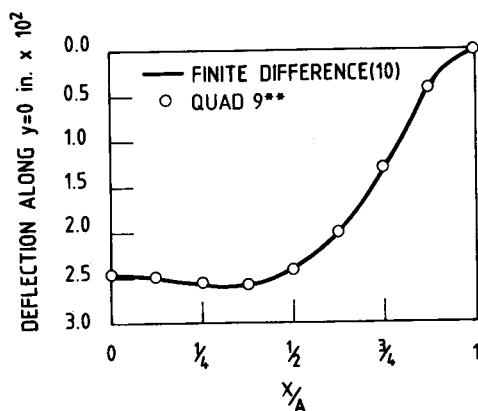


Figure 11. Deflection at centre-line of hyperbolic shell

Table IV. The distribution of transverse displacement along the central line in a clamped hyperbolic shell—comparison of results from QUAD9** and QUAD9*F with 2×2 , 4×4 and 8×8 meshes

Mesh	x/a	QUAD9**	QUAD9*F	Exact solution
2×2	0.000	5.3859	5.3853	
4×4	0.000	2.3790	2.3956	
8×8	0.000	2.4212	2.4185	2.46
	0.125	2.4632	2.4608	
	0.250	2.5455	2.5440	
	0.375	2.5804	2.5800	
	0.500	2.4402	2.4403	
	0.625	2.0036	2.0039	
	0.750	1.2865	1.2864	
	0.875	0.4394	0.4391	
	1.000	0.0	0.0	

CONCLUSIONS

The new shell element with enhanced strain interpolation which is studied in this paper has neither shear locking nor membrane locking. The new shell element, which has no mechanisms, can be used for thick and thin shell structures.

The new shell element with the enhanced interpolation of membrane strains can be used for analyses of problems with either material or geometrical non-linearities, whereas the Lagrange element with selective integration for the membrane stiffness can only be used when the material properties of shell are constant through the thickness or vary symmetrically about shell the midsurface.

A new 8-node shell element was also developed with the same assumptions. The difference is that for the 8-node element the substitute shear strains are interpolated at 5 points respectively [also see the Appendix] and the unidirectional reduced integration for the membrane stiffness is conducted at the 5 points as well.

APPENDIX. NEW 8-NODE SHELL ELEMENT

To avoid tedious tensor transformations, the following interpretation is presented. Since

$$\begin{aligned}\gamma_{\xi\xi} &= u_{,\xi}^* + w_{,\xi}^* \\ \gamma_{\eta\xi} &= v_{,\xi}^* + w_{,\eta}^*\end{aligned}\quad (48)$$

where u^* , v^* , w^* are displacements defined in the natural system. Because $w_{,\xi}^* = 0$,

$$w^* = w^*(\xi, \eta) = w^*(1, \xi, \eta, \xi\eta, \xi^2, \eta^2, \xi^2\eta, \xi^2\eta^2)$$

and

$$w_{,\xi}^* = w_{,\xi}^*(1, \xi, \eta, \xi\eta, \eta^2, \xi\eta^2) \quad (49)$$

From the main shell assumption, u^* is a linear function of ξ , so that

$$u_{,\xi}^* = u_{,\xi}^*(1, \xi, \eta, \xi\eta, \xi^2, \eta^2, \xi^2\eta, \xi^2\eta^2) \quad (50)$$

Similarly

$$w_{,\eta}^* = w_{,\eta}^*(1, \xi, \eta, \xi\eta, \xi^2, \xi^2\eta) \quad (51)$$

$$v_{,\xi}^* = v_{,\xi}^*(1, \xi, \eta, \xi\eta, \xi^2, \eta^2, \xi^2\eta, \xi\eta^2, \xi^2\eta^2) \quad (52)$$

In this case the polynomial terms for $u_{,\xi}^*$ and $w_{,\xi}^*$ for $v_{,\xi}^*$ and $w_{,\eta}^*$ do not match, whereas clearly they should have the same polynomial terms for thin shell situations.⁶

The differences between the new 9-node and 8-node elements are that the interpolations of transverse shear and membrane strains have different functions.⁶ In the 8-node element, for the transverse shear strains

$$u_{,\xi}^* = u_{,\xi}^*(1, \xi, \eta, \xi\eta, \xi^2, \eta^2, \xi^2\eta, \xi\eta^2) \quad (53)$$

$$w_{,\xi}^* = w_{,\xi}^*(1, \xi, \eta, \xi\eta, \eta^2) \quad (54)$$

$$v_{,\xi}^* = v_{,\xi}^*(1, \xi, \eta, \xi\eta, \xi^2, \eta^2, \xi^2\eta, \xi\eta^2) \quad (55)$$

$$w_{,\eta}^* = w_{,\eta}^*(1, \xi, \eta, \xi\eta, \xi^2) \quad (56)$$

and for the membrane strains

$$u'_{0,x'} = u'_{0,x'}(1, x', y', x'y', (y')^2) \quad (57)$$

$$v'_{0,y'} = v'_{0,y'}(1, x', y', x'y', (x')^2) \quad (58)$$

$$u'_{0,y'} = u'_{0,y'}(1, x', y', x'y', (x')^2) \quad (59)$$

$$v'_{0,x'} = v'_{0,x'}(1, x', y', x'y', (y')^2) \quad (60)$$

REFERENCES

1. S. Ahmad, 'Curved finite elements in the analysis of solid, shell and plate', *Ph.D. Thesis*, University College of Swansea, C/PH/7/69.
2. O. C. Zienkiewicz, R. L. Taylor and J. M. Too, 'Reduced integration techniques in general analysis of plates and shells', *Int. j. num. methods eng.*, **3**, 275-290 (1971).
3. E. Onate, E. Hinton and N. Glover, 'Techniques for improving the performance of Ahmad shell elements', *Proc. Int. Conf. on Applied Numerical Modelling*, Madrid, Pentech Press, 1978.
4. K. J. Bathe and E. N. Dvorkin, 'A four-node plate bending element based on Mindlin/Reissner plate theory and a mixed interpolation', *Int. j. num. methods eng.*, **21**, 367-383 (1985).
5. E. N. Dvorkin and K. J. Bathe, 'A continuum mechanics based four-node shell element for general nonlinear analysis', *Eng. Comput.*, **1**, 77-88 (1984).
6. H. C. Huang and E. Hinton, 'A nine node Lagrangian Mindlin plate element with enhanced shear interpolation', *Eng. Comput.*, **1**, 369-379 (1984).
7. R. D. Mindlin, 'Influence of rotary inertia and shear on flexural motions of isotropic, elastic plate', *J. Appl. Mech.*, **18**, 31-38 (1951).
8. H. Parisch, 'A critical survey of the 9-node degenerated shell element with special emphasis on thin shell application and reduced integration', *Comp. Meth. Appl. Mech. Eng.*, **20**, 323-350 (1979).
9. J. J. Connor and C. Brebbia, 'Stiffness matrix for shallow rectangular shell element', *J. Eng. Mech. Div. ASCE*, **93**, (EM5), 43-45 (1967).
10. K. J. Bathe, *Finite Element Procedures in Engineering Analyses*, Prentice-Hall, Englewood Cliffs, New Jersey, 1982.
11. T. J. R. Hughes and M. Cohen, 'The "Heterosis" finite element for plate bending', *Computers and Structures*, **9**, 445-450 (1978).
12. K. Forsberg, 'An evaluation of finite element techniques for general shell', *Symposium on High Speed Computing of Elastic Structure*, I.U.T.A.M., Liege, 1970.
13. H. C. Huang and E. Hinton, 'An improved Lagrangian 9-node Mindlin plate element', *Proc. NUMETA 85*, University College of Swansea, January 1985, Balkema, Amsterdam, 1985.
14. G. M. Lindberg, M. D. Olson and G. R. Cowper, 'New developments in the finite element analysis of shells', *Quarterly Bulletin of the Divisions of Mech. Eng. and the Natural Aeronautical Establishment*, Natural Research Council of Canada, **4**, 1969.
15. N. Flugge, 'Stresses in Shells', Springer-Verlag, Berlin, 1962, pp. 221-226.
16. E. Hinton and H. C. Huang, 'A family of quadrilateral Mindlin plate elements with substitute shear strain fields', Submitted to *Computers and Structures*.
17. E. D. L. Pugh, E. Hinton and O. C. Zienkiewicz, 'A study of quadrilateral plate bending elements with "reduced" integration', *Int. j. num. methods eng.*, **12**, 1059-1079 (1978).